THE JOURNAL OF BIOLOGICAL CHEMISTRY VOL. 287, NO. 31, pp. 26400–26408, July 27, 2012

Multifaceted Recognition of Vertebrate Rev1 by Translesion Polymerases ζ and κ*

Received for publication, May 11, 2012, and in revised form, June 11, 2012 Published, JBC Papers in Press, June 14, 2012, DOI 10.1074/jbc.M112.380998

Jessica Wojtaszek[‡1], Jiangxin Liu[‡1], Sanjay D'Souza[§1], Su Wang[‡], Yaohua Xue[¶], Graham C. Walker[§], and Pei Zhou[‡2]

From the [‡]Department of Biochemistry, Duke University, Medical Center, Durham, North Carolina 27710, the [§]Department of Biology, Massachusetts Institute of Technology, Cambridge, Massachusetts 02139, and the [¶]Trinity College of Arts & Sciences, Duke University, Durham, North Carolina 27708

Background: Translesion synthesis requires the scaffolding function of the Rev1 CTD.
Results: We determined the structures of the Rev1 CTD and its complex with Pol κ and mapped its Rev7-binding surface.
Conclusion: Distinct surfaces of the Rev1 CTD separately mediate the assembly of extension and insertion translesion polymerase complexes.
Significance: Cancer therapeutics could be developed by inhibiting Rev1 CTD-mediated translesion synthesis.

Translesion synthesis is a fundamental biological process that enables DNA replication across lesion sites to ensure timely duplication of genetic information at the cost of replication fidelity, and it is implicated in development of cancer drug resistance after chemotherapy. The eukaryotic Y-family polymerase Rev1 is an essential scaffolding protein in translesion synthesis. Its C-terminal domain (CTD), which interacts with translesion polymerase ζ through the Rev7 subunit and with polymerases κ, ι, and η in vertebrates through the Rev1-interacting region (RIR), is absolutely required for function. We report the first solution structures of the mouse Rev1 CTD and its complex with the Pol κ RIR, revealing an atypical four-helix bundle. Using yeast two-hybrid assays, we have identified a Rev7-binding surface centered at the α2-α3 loop and N-terminal half of α3 of the Rev1 CTD. Binding of the mouse Pol κ RIR to the Rev1 CTD induces folding of the disordered RIR peptide into a three-turn α-helix, with the helix stabilized by an N-terminal cap. RIR binding also induces folding of a disordered N-terminal loop of the Rev1 CTD into a β-hairpin that projects over the shallow α1-α2 surface and creates a deep hydrophobic cavity to interact with the essential FF residues juxtaposed on the same side of the RIR helix. Our combined structural and biochemical studies reveal two distinct surfaces of the Rev1 CTD that separately mediate the assembly of extension and insertion translesion polymerase complexes and provide a molecular framework for developing novel cancer therapeutics to inhibit translesion synthesis.

An alarming number of DNA lesions are generated continually in living cells from endogenous cellular processes and from exposure to exogenous genotoxic agents (1, 2). DNA lesions that have escaped from sophisticated DNA repair mechanisms such as nucleotide and base excision repair cannot be utilized as a template by high-fidelity replicative DNA polymerases, resulting in blockage of the replication fork and formation of replication gaps. To promote cell survival and complete DNA replication before mitosis, cells employ specialized DNA polymerases to bypass lesions in a damage tolerance process known as translesion synthesis at the cost of replication fidelity (3, 4).

Translesion synthesis in mammalian cells is carried out by four Y-family polymerases, Pol[3] κ, Pol ι, Pol η, and Rev1, and one heterodimeric B-family polymerase Pol ζ that consists of the Rev3 catalytic subunit and the Rev7 accessory subunit. Accumulating evidence suggests that translesion synthesis is often achieved in a two-step fashion, with one set of polymerases carrying out insertion opposite the lesion followed by a second set of polymerases carrying out the extension (5). The insertion step is achieved by one of the Y-family polymerases κ, ι, η, or Rev1, with each specialized at bypassing distinct lesions (cognate lesions) for optimal replication accuracy (4). In addition to cognate lesions, these insertion polymerases can also bypass a variety of other lesions, often redundantly, though with elevated mutagenic rates. In contrast, many of the translesion synthesis events require the action of the Rev1-Pol ζ complex for efficient primer extension regardless of lesion types (5). Accordingly, deletions of *REV1* and genes encoding the subunits of Pol ζ, *REV3*, and *REV7*, exhibit reduced spontaneous mutation rates and are severely defective for mutations induced by a wide variety of DNA-damaging agents (6–8). Recently, translesion synthesis has also been shown to function in replication-coupled DNA interstrand cross-link repair in a Pol ζ-dependent manner (9), and monoubiquitinated Rev1 has been found to interact with the Fanconi anemia core complex, providing a critical link between the Fanconi anemia pathway and

* This work was supported by grants from the National Institutes of Health, NIGMS GM-079376 and Stewart Trust Foundation (to P. Z.) and National Institutes of Health, NIEHS ES-015818 and an American Cancer Society Research professorship (to G. C. W.).

The chemical shifts and NMR constraints have been deposited to the BioMagResBank under accession nos. 18431 and 18433 for the mRev1 CTD and the mRev1 CTD-mPol κ RIR complex, respectively.

The atomic coordinates and structure factors (codes 2LSG and 2LSJ) have been deposited in the Protein Data Bank, Research Collaboratory for Structural Bioinformatics, Rutgers University, New Brunswick, NJ (http://www.rcsb.org/).

[1] These authors contributed equally to this work.

[2] To whom correspondence should be addressed: Dept. of Biochemistry, Duke University Medical Center, Durham, NC 27710. Tel.: 919-668-6409; Fax: 919-684-8885; E-mail: peizhou@biochem.duke.edu.

[3] The abbreviations used are: Pol, polymerase; CTD, C-terminal domain; RIR, Rev1-interacting region; mRev1, mouse Rev1; r.m.s.d., root mean square deviation; PCNA, proliferating cell nuclear antigen.

translesion synthesis activity (10). These results have further expanded the function of translesion synthesis and highlight the fundamental roles of Rev1 and Pol ζ in this biologically important process.

The overlapping phenotype of *rev1* and *rev3* mutants in yeast has long implicated a functional connection between Rev1 and Pol ζ, although their physical interaction has only been established recently (11–14). The binding between Rev1 and Pol ζ has been mapped to the C-terminal domain (CTD) of ~100 residues of Rev1 and the Rev7 subunit of Pol ζ. Accordingly, the Rev1 CTD has been shown to play an essential role in cell survival following UV irradiation and exposure to DNA-damaging agents such as methyl methanesulfonate or cisplatin in yeast and vertebrate cells (14, 15).

In vertebrates, but not in lower eukaryotes such as *Saccharomyces cerevisiae*, the Rev1 CTD has also been shown to interact with disordered Rev1-interacting regions (RIRs) of Y-family polymerases κ, ι, and η (12, 13, 16, 17). Such interactions are functionally important for Pol κ and Pol η activity in translesion synthesis. For example, the protective effect of Pol κ against benzo[a]pyrene in mammalian cells requires the binding of the Pol κ RIR and Rev1 (18, 19); in addition, the Rev1-Pol η RIR interaction promotes nuclear accumulation of Rev1 at sites of UV irradiation and helps suppress spontaneous mutations in human cells (20).

Despite its essential role in translesion synthesis, there has been no structural information about the Rev1 CTD or its complex with other translesion polymerases. As a first step toward understanding the molecular basis of the Rev1-mediated assembly of translesion polymerase complexes, we have determined the solution structures of the mouse Rev1 (mRev1) CTD and its complex with the RIR of mouse Pol κ (mPol κ), and have mapped its binding interface toward the Rev7 subunit of Pol ζ using yeast two-hybrid assays. Our structural and biochemical studies reveal two distinct but adjacent binding surfaces of the mRev1 CTD that separately interact with Pol ζ and the RIRs of insertion polymerases in translesion synthesis.

EXPERIMENTAL PROCEDURES

Molecular Cloning and Protein Purification—The NMR constructs contain the mRev1 CTD of 100 residues (1150–1249) or 115 residues (1135–1249) cloned into a modified pMAL-C2 vector (New England Biolabs) to yield a His_6-MBP-tagged protein with a TEV site between MBP and the Rev1 CTD. The mPol κ RIR constructs of 546–616 and 560–582 were cloned into a modified pET15b vector (EMD Biosciences) to produce His_{10}-GB1-tagged protein with a TEV site between GB1 and the RIR.

The His_6-MBP-tagged Rev1 CTD was overexpressed in GW6011 *Escherichia coli* cells, induced with 0.1 mM isopropyl 1-thio-β-D-galactopyranoside at 18 °C for 18 h, and purified by nickel-nitrilotriacetic acid affinity chromatography. After TEV digestion to remove the His_6-MBP tag, the Rev1 CTD was further purified by size-exclusion chromatography. The mPol κ RIR was overexpressed in BL21(DE3)STAR *E. coli* cells, induced with 1 mM isopropyl 1-thio-β-D-galactopyranoside at 37 °C for 6 h, and purified following a similar procedure as the mRev1 CTD. The mRev1 CTD-Pol κ RIR complex was prepared by co-purification. Isotopically enriched proteins were overexpressed in M9 media using ^{15}N-NH_4Cl and ^{13}C-glucose as the sole nitrogen and carbon sources (Cambridge Isotope Laboratories). NMR buffers contain 25 mM sodium phosphate, 100 mM KCl, and 10% D_2O or 100% D_2O (pH 7.0).

NMR Spectroscopy—NMR experiments were conducted using Agilent INOVA 600 or 800 MHz spectrometers at 25 °C and 37 °C for the mRev1 CTD and the mRev1 CTD-Pol κ RIR complex, respectively. Backbone resonances were assigned based on standard three-dimensional triple-resonance experiments (21), and side chain resonances were assigned using sparsely sampled high-resolution four-dimensional HCCH-TOCSY and four-dimensional HCCONH TOCSY experiments (22). Distance constraints were derived from high-resolution three-dimensional ^{15}N- or ^{13}C-separated NOESY-HSQC experiments and from sparsely sampled four-dimensional ^{13}C-HMQC-NOESY-^{15}N-HSQC and four-dimensional ^{13}C-HMQC-NOESY-^{13}C-HSQC experiments. NMR data were processed by NMRpipe (23) and analyzed with Sparky (24). NOE cross-peaks were analyzed with a combination of manual and automated assignments and converted into distance constraints using the calibration module in CYANA (25). Dihedral angles were derived from TALOS+ analysis of chemical shift information (26) and from analysis of local NOE patterns. Structural ensembles were generated with CYANA (25). The final structural ensembles (20 structures) of the mRev1 CTD and the mRev1 CTD-Pol κ RIR complex display with no NOE violations >0.5 Å and no dihedral angle violations >5°. The quality of these structures can be evaluated in Tables 1 and 2.

Yeast Two-hybrid Analysis—Protein-protein interactions in the yeast two-hybrid system were performed in the PJ69–4A strain of yeast (27). The mRev1 CTD(1150–1249) and mRev7 harboring the previously described R124A substitution (28) were cloned into the pGAD-C1 (GAL4 activation domain) and pGBD-C1 (GAL4 DNA-binding domain) plasmids marked with leucine and tryptophan, respectively. The assay was performed by growing strains harboring the two plasmids in 3 ml of media lacking leucine and tryptophan for 2 days at 30 °C and spotting 5 μl of cells on selective medium plates lacking leucine and tryptophan (−LW) and on medium also lacking adenine and histidine (−AHLW) to score positive interactions. Interactions were scored after 3 days of growth at 30 °C. Site-directed mutations were generated using the QuikChange protocol (Stratagene) and verified by sequencing.

RESULTS

Rev1 CTD Adopts Atypical Four-helix Bundle—After extensive screening for Rev1 CTD constructs, we have identified the mRev1 CTD(1150–1249) with a cleavable His_6-MBP tag as the optimal construct for structural characterization by NMR. With the exception of disordered residues at the N terminus, the mRev1 CTD is well structured, with mean pairwise r.m.s.d. of 0.47 and 0.94 Å for the backbone and heavy atoms, respectively (Fig. 1*A*). The detailed statistics on the structural ensemble are given in Table 1.

The structure of the mRev1 CTD contains an atypical four-helix bundle consisting of mixed parallel and anti-parallel helices (Fig. 1*B*). Starting from α1 (Phe^{1163}–Thr^{1175}) in a down-

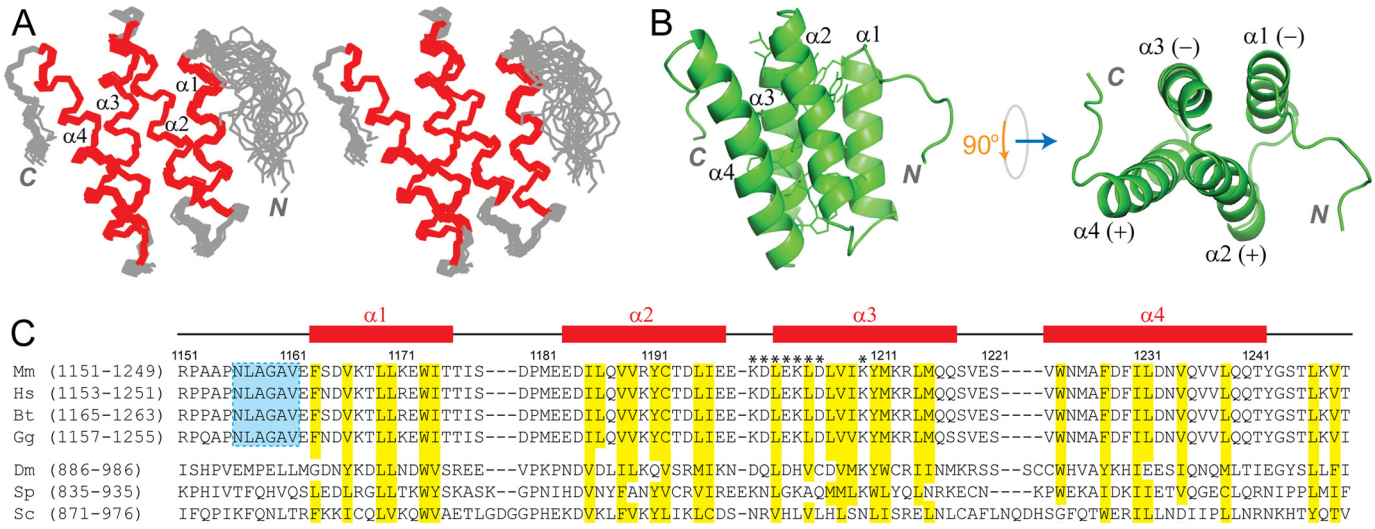

FIGURE 1. **Structure of the mRev1 CTD.** *A*, stereo view of backbone traces from the structural ensemble of the mRev1 CTD, with helices colored in *red* and loops in *gray*. *B*, ribbon diagram. Conserved hydrophobic residues are shown in the stick model (*left panel*). The − sign indicates helices pointing away, whereas the + sign indicates helices pointing inward (*right panel*). *C*, sequence alignment of the Rev1 CTD. Listed species include *Mus musculus* (*Mm*), *Homo sapiens* (*Hs*), *Bos taurus* (*Bt*), *Gallus gallus* (*Gg*), *Drosophila melanogaster* (*Dm*), *S. pombe* (*Sp*), and *S. cerevisiae* (*Sc*). Conserved hydrophobic residues are colored in *yellow*. Disordered mRev1 CTD residues that undergo RIR binding-induced folding are *boxed* in *blue*. Residues important for Rev7 binding are denoted by *asterisks*. *C*, C-terminal; *N*, N-terminal.

TABLE 1

Structural statistics for the mRev1 CTD (20 structures)

None of these structures exhibit distance violations >0.5 Å or dihedral angle violations >5°.

NOE distance restraints (total)	2262
Intra-residue	610
Sequential	545
Medium range ($1< \|i-j\| \leq 4$)	666
Long range ($\|i-j\| \geq 5$)	441
Dihedral angle constraints[a]	160
Target function value	0.46 ± 0.11
Ramachandran plot[b]	
Favored region (98%)	97.2
Allowed region (>99.8%)	99.9
Mean pairwise r.m.s.d. (residues 1163–1249)	
Backbone	0.47 ± 0.10 Å
Heavy atoms	0.94 ± 0.09 Å

[a] Dihedral angle constraints were generated by TALOS+ based on backbone atom chemical shifts and by analysis of NOE patterns (26).
[b] MolProbity was used to assess the quality of the structures (52).

ward orientation and connected by a long, seven-residue loop, α2 (Glu^{1183}–Glu^{1197}) is positioned to the left of α1 in an upward, anti-parallel orientation. Followed by a short three-residue loop across space, α2 connects into a downward oriented α3 (Leu^{1201}–Gln^{1217}) located adjacent to and packed parallel with α1. Helices α3 and α4 (Val^{1222}–Thr^{1241}) are connected by a short loop of four residues, with α4 positioned adjacent to α2 and α3 and pointing upward. The longest helix α4 is tilted at a small angle of ~20° with respect to α2 and α3 and is oriented largely parallel with α2 and anti-parallel with α3.

Similar to the formation of other four-helix bundles, packing of the mixed parallel and anti-parallel four-helix bundle of the mRev1 CTD involves an interaction network of hydrophobic residues among individual helices, including Phe^{1163}, Val^{1166}, Leu^{1170}, Trp^{1173}, Ile^{1174} of α1, Ile^{1185}, Val^{1188}, Val^{1189}, Tyr^{1191}, Cys^{1192}, Leu^{1195}, Ile^{1196} of α2, Leu^{1201}, Leu^{1204}, Val^{1207}, Ile^{1208}, Met^{1211}, Leu^{1214}, and Met^{1215} of α3, and Trp^{1223}, Phe^{1227}, Leu^{1231}, Val^{1234}, and Leu^{1238} of α4 that collectively form an extended hydrophobic core (Fig. 1*B*). In addition to the central four-helix bundle, the residues C-terminal to α4 form an extended β-loop, with the side chains of Leu^{1246} and Val^{1248} juxtaposed to interact with the exposed hydrophobic surface between α3 and α4. The vast majority of these hydrophobic residues are highly conserved from yeast to human (Fig. 1*C*), supporting the existence of a stable protein module in the Rev1 CTD across different species.

Intriguingly, compared with typical four-helix bundle proteins containing equally spaced helices, the location of α1 in the mRev1 CTD is much closer to α3 than to α2. This creates an extended, solvent exposed hydrophobic surface that is optimal for interaction with other proteins. Query of the Dali Server (29) did not reveal a similar fold of isolated four-helix bundles with r.m.s.d. <4 Å or Z-score >5. However, a similar topology can be found as part of seven-helix bundle proteins (*e.g.* CID of PCF11, Protein Data Bank code 2BF0) to interact with other structural elements, reinforcing the notion that the Rev1 CTD is ideally suited as a scaffolding protein.

Rev7 Recognition Surface Centers at α2-α3 Loop and α3 Helix of Rev1 CTD—Having elucidated the structure of the mRev1 CTD, we next probed its interaction with the Rev7 subunit of Pol ζ using yeast two-hybrid assays. The mRev1 CTD and mouse Rev7 (mRev7) containing a R124A substitution, thought to stabilize its closed conformation (28), were fused to either the activation domain or the DNA-binding domain of the Gal4 transcription factor, respectively. Reciprocally, we also appended the mRev1 CTD to the DNA-binding domain and mRev7 to the activation domain of Gal4. The presence of the constructs after transformation into the PJ69-4A strain of yeast was verified by growth on selective medium plates lacking leucine and tryptophan (−LW). Interactions between the two proteins activate the expression of the *HIS3* and *ADE2* reporter genes, both driven by promoters responsive to the Gal4 transcription factor. These interactions were scored by growth on selective medium plates additionally lacking adenine and histi-

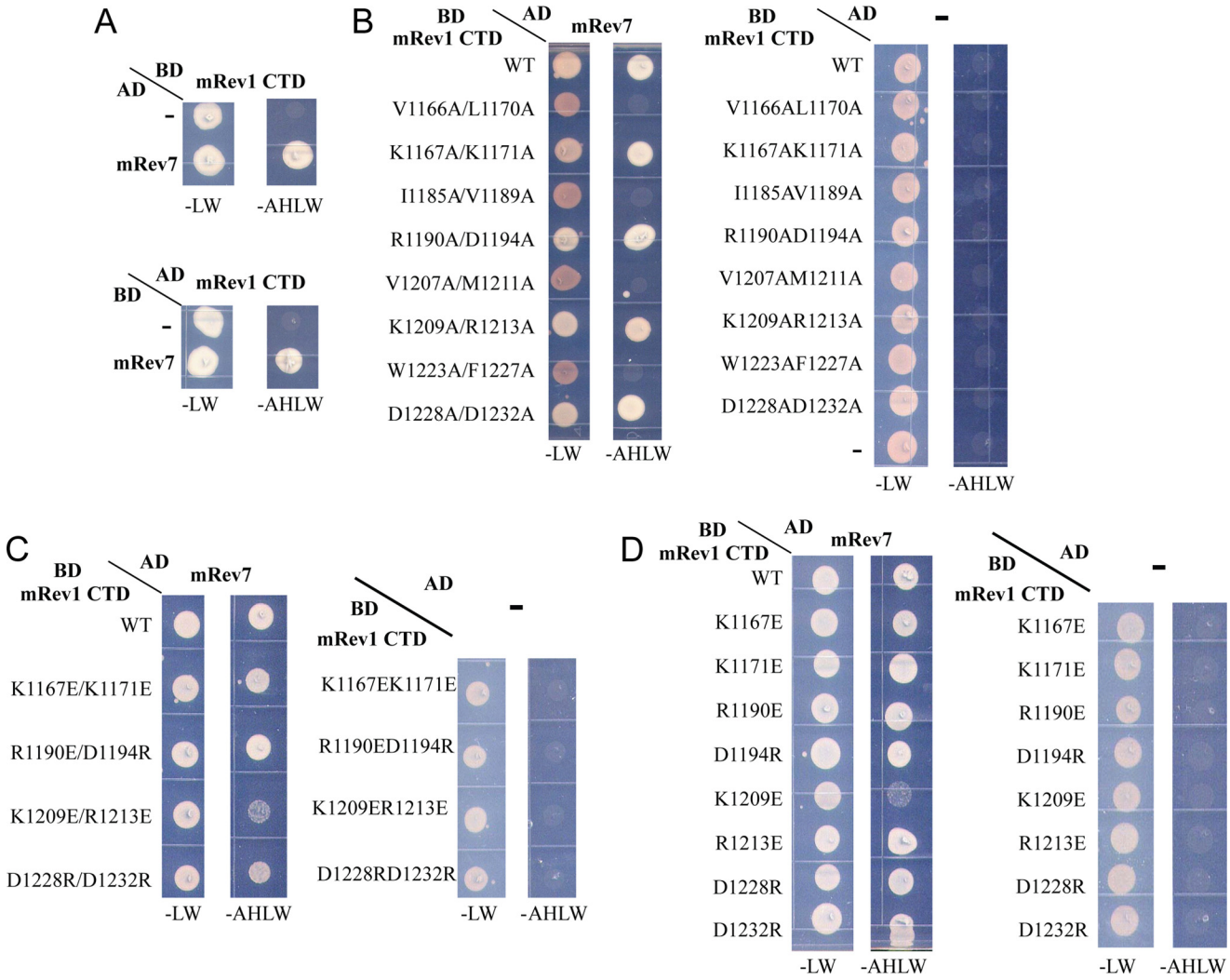

FIGURE 2. **Interactions between the mRev1 CTD and mRev7 probed by yeast two-hybrid assays.** *A*, mRev1 CTD interacts with mRev7. Plasmids containing the mRev1 CTD fused to the *GAL4* DNA-binding domain (*BD*, *upper panel*) or the activation domain (*AD*, *lower panel*) were transformed into strains harboring mRev7 fused to the activation domain (*upper panel*) or DNA-binding domain (*lower panel*) or into strains harboring empty expression plasmids (indicated by the − sign). The plasmids were selected for on −LW plates and interactions scored by growth on −AHLW selective medium plates. *B*, mutations in the mRev1 CTD affect mRev7 binding. *C*, hydrophilic residues in the mRev1 CTD mediate mRev7 interaction. *D*, Lys^{1209} in the mRev1 CTD interacts with mRev7. In *B–D*, interaction between the *GAL4* DNA-binding domain-mRev1 CTD containing indicated mutations and *GAL4* activation domain-mRev7 were monitored using yeast two-hybrid assays as described in *A*. The − indicate control reactions in which *GAL4* DNA-binding domain-fused mRev1 CTD plasmids were transformed into strains harboring the *GAL4* activation domain empty expression vector.

dine (−AHLW). Consistent with published data (12), the interaction between the mRev1 CTD and mRev7 resulted in robust growth of strains in selective media lacking AHLW when either protein was fused to the activation domain or DNA-binding domain of Gal4; in contrast, no growth was observed in strains expressing the mRev1 CTD and empty expression plasmids, verifying that the Rev1 CTD-Rev7 interaction is specific (Fig. 2*A*).

After establishing a strong interaction between the mRev1 CTD and mRev7, in an effort to identify "hot spot" residues that contribute prominently to the binding energy, we mutated pairs of residues of the mRev1 CTD and evaluated their interactions with mRev7 in yeast two-hybrid assays using the mRev1 CTD fused to the DNA-binding domain and mRev7 appended to the activation domain of Gal4.

We first evaluated the effect of mutating pairs of highly conserved hydrophobic residues of individual helices of the mRev1 CTD (Fig. 2*B*). Double mutations of V1166A/L1170A within α1, I1185A/V1189A of α2, V1207A/M1211A of α3, or W1223A/F1227A of α4 abrogated the mRev1 CTD interaction with mRev7. Because these residues form the hydrophobic core of the mRev1 CTD, their substitutions by alanine likely disrupted the proper folding of the mRev1 CTD and thus its interaction with mRev7.

We next evaluated the contribution of surface exposed hydrophilic residues of individual helices toward Rev7 binding, using double alanine substitutions or mutations that result in single- or double-charge reversion (Fig. 2, *B–D*). None of the double-alanine substitutions (K1167A/K1171A of α1, R1190A/D1194A of α2, K1209A/R1213A of α3, or D1228A/D1232A of α4) disrupted the mRev1 CTD-Rev7 binding. Although single- or double-charge reversion mutants on α1 (K1167E, K1171E, K1167E/K1171E), α2 (R1190E, D1194R, R1190E/D1194R) or α4 (D1228R, D1232R, D1228R/D1232R) of the mRev1 CTD

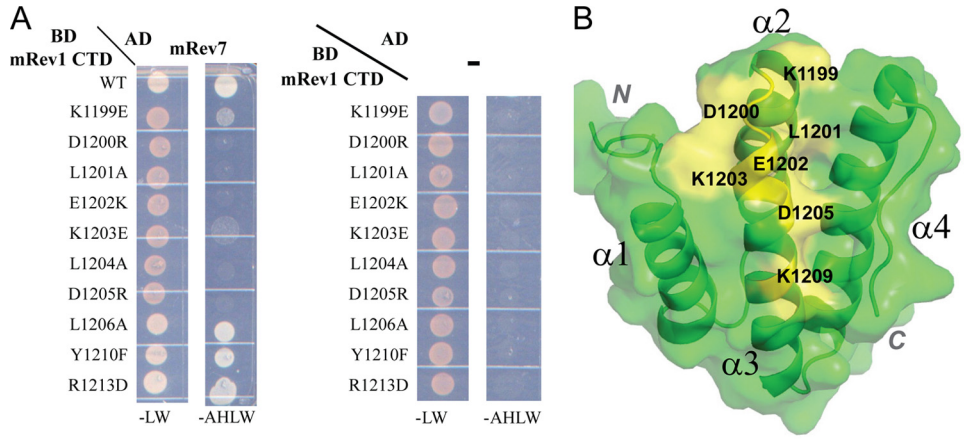

FIGURE 3. **mRev7 binds to the mRev1 CTD primarily through a surface centered at the α2–α3 loop and the N-terminal part of α3.** *A*, interactions of the *GAL4* DNA-binding domain-fused mRev1 CTD harboring indicated mutations with *GAL4* activation domain-mRev7 probed by yeast two-hybrid assays as described in Fig. 2*A*. The − indicates control reactions in which *GAL4* DNA-binding domain-fused mRev1 CTD plasmids were transformed into strains harboring the *GAL4* activation domain empty expression vector. AD denotes the *GAL4* activation domain, and *BD* denotes the *GAL4* DNA-binding domain. *B*, surface mapping of the mRev1 CTD residues important for mRev7 interaction.

had little effect on Rev7 binding, substitutions of positively charged Lys^{1209}/Arg^{1213} of α3 with negatively charged glutamate residues resulted in a significant reduction of the mRev1 CTD-Rev7 binding (Fig. 2, *C* and *D*). Interestingly, mutation of K1209E, but not R1213E, of α3 severely compromised the interaction with Rev7 in yeast two-hybrid assays, suggesting that Lys^{1209} in α3 of the mRev1 CTD is directly involved in Rev7 binding.

To more specifically delineate mRev1 CTD residues important for Rev7 binding, we engineered a set of mutations that span the α2-α3 loop and α3 of the mRev1 CTD and tested their ability to disrupt the Rev7 interaction (Fig. 3*A*). Mutations of hydrophobic residues (L1201A or L1204A) involved in packing of the four-helix bundle disrupted the mRev1 CTD-Rev7 interaction, whereas mutations of Y1210F and L1206A had no effect. Mutation of R1213D, a surface exposed hydrophilic residue at the C-terminal end of α3 also did not affect the mRev1 CTD-Rev7 interaction, suggesting that the mRev1 CTD recognition by Rev7 is mediated by the N-terminal half of α3 of the mRev1 CTD. Consistent with this notion, single amino acid substitutions of hydrophilic residues at the N-terminal part of α3 containing an opposite charge (E1202K, K1203E, or D1205R) completely abolished the Rev7 interaction. Additionally, point mutations of K1199E and D1200R located in the loop connecting α2 and α3, either significantly reduced or abolished the Rev7 interaction. No binding was observed in control experiments between the mRev1 CTD harboring these mutations and an empty expression plasmid, verifying the specificity of these interactions in our assays. Taken together, these results define the α2-α3 loop and the N-terminal half of α3 of the Rev1 CTD as the primary Rev7-binding site (Fig. 3*B*).

A Minimal RIR of Pol κ for Rev1 Interaction—The interactions between vertebrate Rev1 and other members of the Y-family polymerases have been mapped to the Rev1 CTD and disordered RIR fragments of ~50 residues within Pol κ, Pol ι, and Pol η (17). Because the RIR of human Pol κ has the tightest binding affinity toward the Rev1 CTD (19), its mouse counterpart was chosen for characterization by NMR. The mPol κ RIR(546–616) displays a typical ^{1}H-^{15}N HSQC spectrum of a disordered peptide, with amide resonances showing a narrow chemical shift distribution. By analyzing mPol κ RIR amide resonances that experience substantial perturbations upon binding to the mRev1 CTD, we have identified a 23-residue RIR peptide of mPol κ(560–582) that not only binds to the mRev1 CTD tightly but also causes identical resonance perturbations for the mRev1 CTD as the longer peptide. This 23-residue peptide was subsequently used to investigate the mRev1 CTD-Pol κ RIR interaction.

Binding-induced Folding of mRev1 CTD and Pol κ RIR—During our studies of the mRev1 CTD, we found that extending the ~100 residue mRev1 CTD construct by 15 residues at the N terminus improved the sample yield and stability. This optimized construct (mRev1(1135–1249)) was used for structural determination of the mRev1 CTD-Pol κ RIR complex. The overall structure of the mRev1 CTD-Pol κ RIR complex is well defined, with mean pairwise r.m.s.d. of 0.42 and 0.89 Å for the backbone and heavy atoms, respectively (Fig. 4*A*). The detailed statistics on the structural ensemble are given in Table 2.

The core helix-bundle structure of the mRev1 CTD in complex with the Pol κ RIR is similar to that of the free protein. However, the six residues N-terminal to α1 (Asn^{1156}–Val^{1161}) are completely disordered in the free Rev1 CTD, whereas binding of the Pol κ RIR induces folding of these residues into a β-hairpin that projects over the shallow hydrophobic surface between α1 and α2 and creates a deep hydrophobic cavity for high-affinity interaction with the essential FF motif of the Pol κ RIR (Fig. 4, *B*–*D*).

The binding of the mRev1 CTD similarly induces folding of the disordered Pol κ RIR into a three-turn α-helix, starting from Phe^{566} and ending at Ile^{575} (Fig. 4). The folding of the RIR helix is stabilized by a prototypical N-helix cap at Ser^{565} (30), with the side chain of Ser^{565} forming hydrogen bonds with amides of Phe^{567} and Asp^{568} and its backbone carbonyl oxygen atom forming another hydrogen bond with the amide of Lys^{569}. Substitution of the corresponding serine residue in human Pol κ RIR by alanine reduced its binding affinity toward Rev1 by more than 50% in a yeast two-hybrid assay (19); however, substitution of serine with proline, another N-helix cap residue, did not

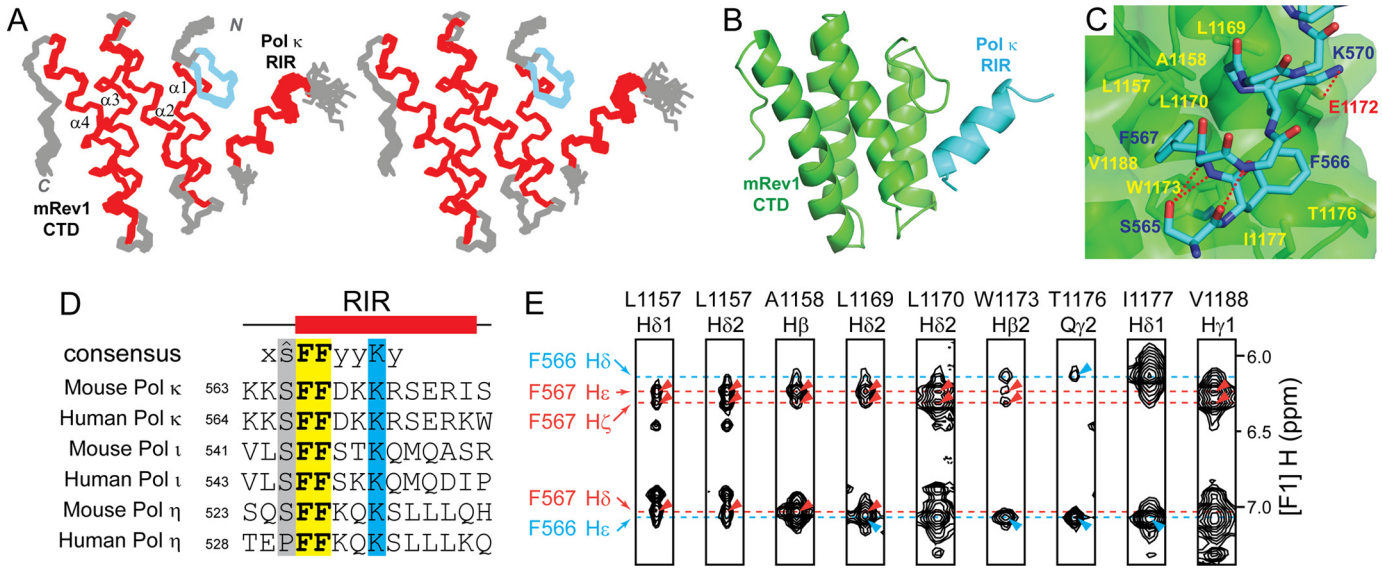

FIGURE 4. **Structure of the mRev1 CTD-Pol κ RIR complex.** *A*, stereo view of backbone traces from the structural ensemble of the mRev1 CTD-Pol κ RIR complex, with helices colored in *red*, loops colored in *gray*, and a six-residue hairpin loop that undergoes a binding-induced folding transition, colored in *blue*. *B*, ribbon diagram, with mRev1 CTD colored in *green* and Pol κ RIR colored in *blue*. *C*, interface of the Rev1 CTD-Pol κ RIR complex. Side chains of conserved Pol κ RIR residues and their binding partners are shown in the stick model. *D*, sequence alignment of RIR peptides from Y-family polymerases κ, ι, and η. Conserved residues are colored, with the essential FF motif highlighted. ŝ refers to a helix cap residue that is predominantly serine but can be replaced by proline. *E*, representative intermolecular NOEs (indicated by *arrows*) between the aromatic side chains of Phe[566] and Phe[567] of the mPol κ RIR and their interacting residues of the mRev1 CTD.

TABLE 2

Structural statistics for the mRev1 CTD-mPol κ RIR (20 structures)

None of these structures exhibit distance violations >0.5 Å or dihedral angle violations >5°.

mRev1 CTD	
NOE distance restraints	3530
Intra-residue	737
Sequential	738
Medium range ($1< \|i-j\| \leq 4$)	1029
Long range ($\|i-j\| \geq 5$)	1026
Dihedral angle constraints[a]	178
mPol κ RIR	
NOE distance restraints	202
Intra-residue	77
Sequential	56
Medium range ($1 <\|i-j\| \leq 4$)	69
Long range ($\|i-j\| \geq 5$)	0
Dihedral angle constraints[a]	24
Intermolecular NOE distance constraints	167
Target function value	1.76 ± 0.09
Ramachandran plot[b]	
Favored region (98%)	97.6
Allowed region (>99.8%)	100.0
Mean pairwise r.m.s.d. (mRev1 CTD 1153–1249; Pol κ 564–576)	
Backbone	0.42 ± 0.09 Å
Heavy Atoms	0.89 ± 0.09 Å

[a] Dihedral angle constraints were generated by talos+ based on backbone atom chemical shifts, and by analysis of NOE patterns (26).
[b] MolProbity was used to assess the quality of the structures (52).

affect Rev1 binding (19), highlighting the important contribution of an N-terminal cap to the stability of this binding-induced RIR helix.

Immediately following Ser[565] are two essential phenylalanine residues Phe[566] and Phe[567] that emanate from the same side of the RIR helix to interact with the Rev1 CTD. The aromatic ring of Phe[566] extends over a hydrophobic surface patch formed by residues Trp[1173], Thr[1176], and Ile[1177] located at the C-terminal end of α1 and the loop immediately following it. The side chain of Phe[567], with its phenyl ring located almost perpendicular to that of Phe[566], wedges into and is completely immersed in a deep hydrophobic pocket of the Rev1 CTD. The base of the hydrophobic pocket is formed by Leu[1170] of α1 and Val[1188] of α2. At one side of the hydrophobic pocket lies the indole ring of the Trp[1173] of α1, whereas the opposite side of the pocket is sealed by the side chains of Leu[1157] and Ala[1158] that project over from the newly forged β-hairpin in response to the binding of the Pol κ RIR. These core hydrophobic interactions are additionally supported by interactions between Phe[567] and the side chain methylene groups of the nearby Gln[1187] of α2. Reflecting their essential role in the Rev1 CTD-RIR interaction, the FF motif is strictly conserved, their strong interactions with the Rev1 CTD are supported by the observation of numerous intermolecular NOEs (Fig. 4*E*), and alanine substitution of either of the FF residues abolishes the Rev1 CTD-RIR interaction (19).

The two residues after Phe[567], Asp[568], and Lys[569] are surface-exposed and are not engaged in Rev1 CTD interaction. In contrast, the following residue, Lys[570] is located on the same side of the RIR helix as the two essential phenylalanine residues, with its side chain extending over the aromatic ring of Phe[566]. A number of intermolecular NOEs can be observed between the side chains of Lys[570] of the Pol κ RIR and Glu[1172] of the mRev1 CTD; additional NOEs between both residues to the aromatic ring of Phe[566] in the Pol κ RIR are also visible, suggesting that these two residues are located in the vicinity of Phe[566] and they are engaged in a specific charge-charge interaction. Reflecting this observation, Lys[570] is highly conserved among vertebrate RIRs that have been shown to interact with the Rev1 CTD.

In addition to these essential and highly conserved interactions, intermolecular NOEs have also been observed between Pol κ RIR residues Lys[564], Arg[571], and Arg[574] and mRev1 CTD residues Met[1181], Ala[1158], and Ala[1160], respectively. Although

these interactions may provide additional support to anchor the Pol κ RIR onto the Rev1 CTD, these RIR residues are not conserved, and they are unlikely to contribute significantly to the binding affinity.

Our structure of the mRev1 CTD-Pol κRIR complex has revealed a binding surface of the Rev1 CTD that consists of α1 and α2 helices and a newly forged N-terminal β-hairpin loop in response to RIR interaction. This structurally defined RIR-binding surface is located adjacent to, but is distinct from, the Rev7-binding surface of the Rev1 CTD centered at the α2–α3 loop and the N-terminal half of the α3-helix as revealed by our yeast two-hybrid studies.

DISCUSSION

Conserved and Acquired Roles of Rev1 CTD in Translesion Synthesis—Rev1 is a unique member of the eukaryotic Y-family polymerases and is conserved from yeast to human. Its gene was identified in a screen for reversionless mutants of *S. cerevisiae* after UV irradiation (6), and it was the first Y-family polymerase that was characterized enzymatically (31). The limited polymerizing ability of Rev1 (31), coupled with the profound effect of the *rev1-1* mutation, which did not affect the catalytic activity of Rev1, led to the proposal of a "second function" of Rev1 in translesion synthesis (32). This second function is now attributed to the scaffolding function of the Rev1 CTD that coordinates recruitment of Pol ζ (14, 33). Deletion of the Rev1 CTD completely abolishes Rev1-dependent translesion synthesis; likewise, elevated levels of the Rev1 CTD show a strong dominant-negative effect on cell viability and induced mutagenesis after DNA damage in yeast (14). Recent studies have revealed a similarly important function of the Rev1 CTD in higher eukaryotes and suggest that the vertebrate Rev1 CTD may have acquired a more prominent role in recruiting Pol ζ and controlling translesion synthesis in the absence of monoubiquitinated PCNA at the stalled replication fork (15, 34). Taken together, these results highlight an essential and highly conserved role of the Rev1 CTD-Pol ζ interaction in translesion synthesis that has now been mapped to the α2–α3 loop and the N-terminal half of the α3-helix in the Rev1 CTD.

In contrast to the Rev1-Pol ζ interaction that is conserved in all eukaryotes, the Rev1 interaction with the RIRs of Pol κ, η, and ι has only been found in vertebrates, but not in *S. cerevisiae* or *Schizosaccharomyces pombe*, suggesting an evolutionary divergence between animals and yeast (17). Because translesion synthesis accounts for <10% of damage bypass events in yeast (35), whereas the frequency of potentially mutagenic translesion synthesis may be as high as 50% in higher eukaryotes (36), it is possible that higher eukaryotic Rev1 have acquired additional interactions with other Y-family polymerases outside the essential Rev7 binding surface to achieve a better regulation of translesion bypass. In this regard, several studies have suggested that in higher eukaryotes, translesion synthesis can be carried out in a PCNA ubiquitination-independent manner (34, 37, 38). In the absence of monoubiquitinated PCNA, which enhances the residence time of translesion polymerases at the replication fork (39), recruitment of the Y-family polymerases κ, η, and ι may particularly benefit from their RIR-mediated interactions with Rev1, which binds independently to PCNA or primer-template junctions of stalled replication forks. The acquired interaction of translesion polymerases κ, η, and ι with the Rev1 CTD may also facilitate the transition from an insertion polymerase complex to the extension polymerase complex of Rev1-Pol ζ after base insertion. Alternatively, given that vertebrates have four Y-family polymerases, each specializing at bypassing a specific type of lesion with relatively high accuracy and efficiency, it is tantalizing to speculate that another function of the Rev1 CTD-RIR interaction is to accelerate the exchange to the correct insertion polymerase if the initially recruited insertion polymerase cannot efficiently bypass the DNA lesion to reduce the error rate of translesion synthesis.

Specificity of Interaction between Rev1 CTD and RIR—Our structure of the mRev1 CTD-Pol κ RIR complex has revealed a surprisingly small binding interface, with the Pol κ RIR forming a short α-helix spanning only ten residues. Apart from Phe^{566}, Phe^{567}, and Lys^{570} of the RIR helix that form specific interactions with the Rev1 CTD and Ser^{565} that serves as an N-terminal helix cap (Fig. 4*D*), the remaining residues are highly variable, and they can be substituted by alanine without affecting the binding affinity toward the Rev1 CTD (19). Interestingly, Lys^{570} can also be substituted by alanine without an obvious effect on binding affinity (19), suggesting that Lys^{570}, despite forming a charge-charge interaction with Glu^{1172} of the mRev1 CTD, does not contribute significantly to the binding energy.

In contrast, the stability of the RIR helix has a significant impact on its binding affinity toward the Rev1 CTD. Substituting the helix cap Ser^{565} by alanine significantly reduced the Rev1 CTD-RIR binding (19); likewise, proline substitution of RIR residues after the FF motif (D568P, K569P, K570P, or R571P) abolished the Rev1 interaction (19), suggesting that the formation of the RIR helix requires a minimum of six residues in addition to a helix stabilizing cap. Such an observation may account for a lack of binding affinity of the Rev1 CTD toward the FF motif found in the PCNA-interacting peptides of Pol κ and Pol η (40). Because the PCNA-interacting peptide of Pol κ contains a single residue after the FF motif, and the PCNA-interacting peptide of Pol η contains a proline residue at the second position after the FF motif, neither is expected to be an effective binding partner of the Rev1 CTD.

Targeting Rev1 CTD-mediated Translesion Synthesis for Cancer Therapy—A hallmark of cancer cells is the accumulation of a vast number of mutations in their genomes (41–43). Cancer-specific mutations have been shown to increase the capacity of cancer cells to carry out mutagenic translesion bypass (44, 45), and extensive mutagenesis in turn contributes to the development of drug resistance in relapsed tumors after chemotherapy (46). The recent discovery that depletion of Rev1 greatly reduces the number of carcinogen-induced lung tumors in mice highlights an important role of translesion synthesis in cancer development (47). In human ovarian carcinoma cells, alteration of the Rev1 level modulates the cytotoxicity and mutagenicity of cisplatin (48, 49). Depletion of Rev1 or Rev3L, the catalytic unit of mouse Pol ζ, sensitizes B-cell lymphomas and chemoresistant lung adenocarcinomas to cisplatin treatment *in vivo* (50). Suppression of Rev1 limits cyclophosphamide-induced mutagenesis *in vitro* and delays the emergence of chemoresistant tumors *in vivo* (50, 51). These studies high-

light the therapeutic potential of inhibiting translesion synthesis in cancer treatment.

Given the essential function of the Rev1 CTD in translesion synthesis, compounds that transiently disrupt the Rev1 CTD-Pol ζ interaction could sensitize cancer cells to DNA damaging therapeutic agents while reducing their mutagenic consequences, suggesting that these compounds may be developed into novel adjuvants to enhance the clinical outcome of current therapies. In this regard, the elucidation of the Rev1 CTD structure and its binding surfaces toward Rev7 and the Pol κ RIR is an important first step toward this goal. Our structural studies have revealed an atypical four-helix bundle fold of the mRev1 CTD, and our yeast genetic data have further identified a set of hot spot residues of the Rev1 CTD and have provided the first residue-specific view of the Rev7-binding interface of the Rev1 CTD, laying a molecular framework for designing novel inhibitors to disrupt the essential and evolutionary conserved Rev1 CTD-Pol ζ interaction. The discovery of multifaceted recognition of the Rev1 CTD by Rev7 and RIR has hinted at the exciting possibility of generating potent inhibitors that separately occupy the Rev7- or RIR-binding surfaces of the Rev1 CTD, which can be used individually or in combination to suppress translesion synthesis. Should these compounds display the desired effectiveness *in vivo*, they could become a novel class of therapeutics to sensitize cancer cells to chemotherapy and to suppress the development of cancer drug resistance.

Acknowledgment—We thank Ashton Lai for assistance with molecular cloning.

REFERENCES

1. Friedberg, E. C., Walker, G. C., Siede, W., Wood, R. D., Schultz, R. A., and Ellenberger, T. (eds). (2005) *DNA Repair and Mutagenesis*, American Society for Microbiology, Washington, DC
2. Lindahl, T., and Barnes, D. E. (2000) Repair of endogenous DNA damage. *Cold Spring Harb. Symp. Quant. Biol.* **65,** 127–133
3. Sale, J. E., Lehmann, A. R., and Woodgate, R. (2012) Y-family DNA polymerases and their role in tolerance of cellular DNA damage. *Nat. Rev. Mol. Cell Biol.* **13,** 141–152
4. Waters, L. S., Minesinger, B. K., Wiltrout, M. E., D'Souza, S., Woodruff, R. V., and Walker, G. C. (2009) Eukaryotic translesion polymerases and their roles and regulation in DNA damage tolerance. *Microbiol. Mol. Biol. Rev.* **73,** 134–154
5. Livneh, Z., Ziv, O., and Shachar, S. (2010) Multiple two-polymerase mechanisms in mammalian translesion DNA synthesis. *Cell Cycle* **9,** 729–735
6. Lemontt, J. F. (1971) Mutants of yeast defective in mutation induced by ultraviolet light. *Genetics* **68,** 21–33
7. Lawrence, C. W., Das, G., and Christensen, R. B. (1985) REV7, a new gene concerned with UV mutagenesis in yeast. *Mol. Gen. Genet* **200,** 80–85
8. Lawrence, C. W. (2004) Cellular functions of DNA polymerase ζ and Rev1 protein. *Adv. Protein Chem.* **69,** 167–203
9. Räschle, M., Knipscheer, P., Knipsheer, P., Enoiu, M., Angelov, T., Sun, J., Griffith, J. D., Ellenberger, T. E., Schärer, O. D., and Walter, J. C. (2008) Mechanism of replication-coupled DNA interstrand cross-link repair. *Cell* **134,** 969–980
10. Kim, H., Yang, K., Dejsuphong, D., and D'Andrea, A. D. (2012) Regulation of Rev1 by the Fanconi anemia core complex. *Nat. Struct. Mol. Biol.* **19,** 164–170
11. Murakumo, Y., Ogura, Y., Ishii, H., Numata, S., Ichihara, M., Croce, C. M., Fishel, R., and Takahashi, M. (2001) Interactions in the error-prone postreplication repair proteins hREV1, hREV3, and hREV7. *J. Biol. Chem.* **276,** 35644–35651
12. Guo, C., Fischhaber, P. L., Luk-Paszyc, M. J., Masuda, Y., Zhou, J., Kamiya, K., Kisker, C., and Friedberg, E. C. (2003) Mouse Rev1 protein interacts with multiple DNA polymerases involved in translesion DNA synthesis. *EMBO J.* **22,** 6621–6630
13. Ohashi, E., Murakumo, Y., Kanjo, N., Akagi, J., Masutani, C., Hanaoka, F., and Ohmori, H. (2004) Interaction of hREV1 with three human Y-family DNA polymerases. *Genes Cells* **9,** 523–531
14. D'Souza, S., Waters, L. S., and Walker, G. C. (2008) Novel conserved motifs in Rev1 C terminus are required for mutagenic DNA damage tolerance. *DNA Repair* **7,** 1455–1470
15. Ross, A. L., Simpson, L. J., and Sale, J. E. (2005) Vertebrate DNA damage tolerance requires the C terminus but not BRCT or transferase domains of REV1. *Nucleic Acids Res.* **33,** 1280–1289
16. Tissier, A., Kannouche, P., Reck, M. P., Lehmann, A. R., Fuchs, R. P., and Cordonnier, A. (2004) Co-localization in replication foci and interaction of human Y-family members, DNA polymerase pol η and REVl protein. *DNA Repair* **3,** 1503–1514
17. Kosarek, J. N., Woodruff, R. V., Rivera-Begeman, A., Guo, C., D'Souza, S., Koonin, E. V., Walker, G. C., and Friedberg, E. C. (2008) Comparative analysis of in vivo interactions between Rev1 protein and other Y-family DNA polymerases in animals and yeasts. *DNA Repair* **7,** 439–451
18. Ogi, T., Shinkai, Y., Tanaka, K., and Ohmori, H. (2002) Polkappa protects mammalian cells against the lethal and mutagenic effects of benzo[a]pyrene. *Proc. Natl. Acad. Sci. U.S.A.* **99,** 15548–15553
19. Ohashi, E., Hanafusa, T., Kamei, K., Song, I., Tomida, J., Hashimoto, H., Vaziri, C., and Ohmori, H. (2009) Identification of a novel REV1-interacting motif necessary for DNA polymerase κ function. *Genes Cells* **14,** 101–111
20. Akagi, J., Masutani, C., Kataoka, Y., Kan, T., Ohashi, E., Mori, T., Ohmori, H., and Hanaoka, F. (2009) Interaction with DNA polymerase η is required for nuclear accumulation of REV1 and suppression of spontaneous mutations in human cells. *DNA Repair* **8,** 585–599
21. Cavanagh, J., Fairbrother, W. J., Palmer, A. G., 3rd, Skelton, N. J., and Rance, M. (2007) *Protein NMR Spectroscopy, Second Edition*: *Principles and Practice*, Elsevier Academic Press, Burlington, MA
22. Coggins, B. E., and Zhou, P. (2008) High resolution four-dimensional spectroscopy with sparse concentric shell sampling and FFT-CLEAN. *J. Biomol. NMR* **42,** 225–239
23. Delaglio, F., Grzesiek, S., Vuister, G. W., Zhu, G., Pfeifer, J., and Bax, A. (1995) NMRPipe: A multidimensional spectral processing system based on UNIX pipes. *J. Biomol. NMR* **6,** 277–293
24. Goddard, T. D., and Kneller, D. G. (2008) *Sparky 3*, Ver. 3.114, University of California, San Francisco, CA
25. Herrmann, T., Güntert, P., and Wüthrich, K. (2002) Protein NMR structure determination with automated NOE assignment using the new software CANDID and the torsion angle dynamics algorithm DYANA. *J. Mol. Biol.* **319,** 209–227
26. Shen, Y., Delaglio, F., Cornilescu, G., and Bax, A. (2009) TALOS+: A hybrid method for predicting protein backbone torsion angles from NMR chemical shifts. *J. Biomol. NMR* **44,** 213–223
27. James, P., Halladay, J., and Craig, E. A. (1996) Genomic libraries and a host strain designed for highly efficient two-hybrid selection in yeast. *Genetics* **144,** 1425–1436
28. Hara, K., Hashimoto, H., Murakumo, Y., Kobayashi, S., Kogame, T., Unzai, S., Akashi, S., Takeda, S., Shimizu, T., and Sato, M. (2010) Crystal structure of human REV7 in complex with a human REV3 fragment and structural implication of the interaction between DNA polymerase ζ and REV1. *J. Biol. Chem.* **285,** 12299–12307
29. Holm, L., and Sander, C. (1993) Protein structure comparison by alignment of distance matrices. *J. Mol. Biol.* **233,** 123–138
30. Lyu, P. C., Wemmer, D. E., Zhou, H. X., Pinker, R. J., and Kallenbach, N. R. (1993) Capping interactions in isolated α helices: Position-dependent substitution effects and structure of a serine-capped peptide helix. *Biochemistry* **32,** 421–425
31. Nelson, J. R., Lawrence, C. W., and Hinkle, D. C. (1996) Deoxycytidyl transferase activity of yeast REV1 protein. *Nature* **382,** 729–731
32. Nelson, J. R., Gibbs, P. E., Nowicka, A. M., Hinkle, D. C., and Lawrence, C. W. (2000) Evidence for a second function for *Saccharomyces cerevisiae*

Rev1p. *Mol. Microbiol.* **37,** 549–554
33. Acharya, N., Johnson, R. E., Prakash, S., and Prakash, L. (2006) Complex formation with Rev1 enhances the proficiency of *Saccharomyces cerevisiae* DNA polymerase ζ for mismatch extension and for extension opposite from DNA lesions. *Mol. Cell. Biol.* **26,** 9555–9563
34. Edmunds, C. E., Simpson, L. J., and Sale, J. E. (2008) PCNA ubiquitination and REV1 define temporally distinct mechanisms for controlling translesion synthesis in the avian cell line DT40. *Molecular cell* **30,** 519–529
35. Baynton, K., Bresson-Roy, A., and Fuchs, R. P. (1998) Analysis of damage tolerance pathways in *Saccharomyces cerevisiae*: A requirement for Rev3 DNA polymerase in translesion synthesis. *Mol. Cell. Biol.* **18,** 960–966
36. Stallons, L. J., and McGregor, W. G. (2010) Translesion synthesis polymerases in the prevention and promotion of carcinogenesis. *J. Nucleic Acids* (2010) pii, 643857
37. Hendel, A., Krijger, P. H., Diamant, N., Goren, Z., Langerak, P., Kim, J., Reissner, T., Lee, K. Y., Geacintov, N. E., Carell, T., Myung, K., Tateishi, S., D'Andrea, A., Jacobs, H., and Livneh, Z. (2011) PCNA ubiquitination is important but not essential for translesion DNA synthesis in mammalian cells. *PLoS Genet.* **7,** e1002262
38. Krijger, P. H., van den Berk, P. C., Wit, N., Langerak, P., Jansen, J. G., Reynaud, C. A., de Wind, N., and Jacobs, H. (2011) PCNA ubiquitination-independent activation of polymerase η during somatic hypermutation and DNA damage tolerance. *DNA Repair* **10,** 1051–1059
39. Sabbioneda, S., Gourdin, A. M., Green, C. M., Zotter, A., Giglia-Mari, G., Houtsmuller, A., Vermeulen, W., and Lehmann, A. R. (2008) Effect of proliferating cell nuclear antigen ubiquitination and chromatin structure on the dynamic properties of the Y-family DNA polymerases. *Mol. Biol. Cell* **19,** 5193–5202
40. Moldovan, G. L., Pfander, B., and Jentsch, S. (2007) PCNA, the maestro of the replication fork. *Cell* **129,** 665–679
41. Lee, W., Jiang, Z., Liu, J., Haverty, P. M., Guan, Y., Stinson, J., Yue, P., Zhang, Y., Pant, K. P., Bhatt, D., Ha, C., Johnson, S., Kennemer, M. I., Mohan, S., Nazarenko, I., Watanabe, C., Sparks, A. B., Shames, D. S., Gentleman, R., de Sauvage, F. J., Stern, H., Pandita, A., Ballinger, D. G., Drmanac, R., Modrusan, Z., Seshagiri, S., and Zhang, Z. (2010) The mutation spectrum revealed by paired genome sequences from a lung cancer patient. *Nature* **465,** 473–477
42. Pleasance, E. D., Cheetham, R. K., Stephens, P. J., McBride, D. J., Humphray, S. J., Greenman, C. D., Varela, I., Lin, M. L., Ordóñez, G. R., Bignell, G. R., Ye, K., Alipaz, J., Bauer, M. J., Beare, D., Butler, A., Carter, R. J., Chen, L., Cox, A. J., Edkins, S., Kokko-Gonzales, P. I., Gormley, N. A., Grocock, R. J., Haudenschild, C. D., Hims, M. M., James, T., Jia, M., Kingsbury, Z., Leroy, C., Marshall, J., Menzies, A., Mudie, L. J., Ning, Z., Royce, T., Schulz-Trieglaff, O. B., Spiridou, A., Stebbings, L. A., Szajkowski, L., Teague, J., Williamson, D., Chin, L., Ross, M. T., Campbell, P. J., Bentley, D. R., Futreal, P. A., and Stratton, M. R. (2010) A comprehensive catalogue of somatic mutations from a human cancer genome. *Nature* **463,** 191–196
43. Pleasance, E. D., Stephens, P. J., O'Meara, S., McBride, D. J., Meynert, A., Jones, D., Lin, M. L., Beare, D., Lau, K. W., Greenman, C., Varela, I., Nik-Zainal, S., Davies, H. R., Ordoñez, G. R., Mudie, L. J., Latimer, C., Edkins, S., Stebbings, L., Chen, L., Jia, M., Leroy, C., Marshall, J., Menzies, A., Butler, A., Teague, J. W., Mangion, J., Sun, Y. A., McLaughlin, S. F., Peckham, H. E., Tsung, E. F., Costa, G. L., Lee, C. C., Minna, J. D., Gazdar, A., Birney, E., Rhodes, M. D., McKernan, K. J., Stratton, M. R., Futreal, P. A., and Campbell, P. J. (2010) A small-cell lung cancer genome with complex signatures of tobacco exposure. *Nature* **463,** 184–190
44. Lin, X., and Howell, S. B. (2006) DNA mismatch repair and p53 function are major determinants of the rate of development of cisplatin resistance. *Mol. Cancer Ther.* **5,** 1239–1247
45. Avkin, S., Sevilya, Z., Toube, L., Geacintov, N., Chaney, S. G., Oren, M., and Livneh, Z. (2006) p53 and p21 regulate error-prone DNA repair to yield a lower mutation load. *Mol. Cell* **22,** 407–413
46. Gottesman, M. M. (2002) Mechanisms of cancer drug resistance. *Annu. Rev. Med.* **53,** 615–627
47. Dumstorf, C. A., Mukhopadhyay, S., Krishnan, E., Haribabu, B., and McGregor, W. G. (2009) REV1 is implicated in the development of carcinogen-induced lung cancer. *Mol. Cancer Res.* **7,** 247–254
48. Lin, X., Okuda, T., Trang, J., and Howell, S. B. (2006) Human REV1 modulates the cytotoxicity and mutagenicity of cisplatin in human ovarian carcinoma cells. *Mol. Pharmacol.* **69,** 1748–1754
49. Okuda, T., Lin, X., Trang, J., and Howell, S. B. (2005) Suppression of hREV1 expression reduces the rate at which human ovarian carcinoma cells acquire resistance to cisplatin. *Mol. Pharmacol.* **67,** 1852–1860
50. Xie, K., Doles, J., Hemann, M. T., and Walker, G. C. (2010) Error-prone translesion synthesis mediates acquired chemoresistance. *Proc. Natl. Acad. Sci. U.S.A.* **107,** 20792–20797
51. Doles, J., Oliver, T. G., Cameron, E. R., Hsu, G., Jacks, T., Walker, G. C., and Hemann, M. T. (2010) Suppression of Rev3, the catalytic subunit of Polζ, sensitizes drug-resistant lung tumors to chemotherapy. *Proc. Natl. Acad. Sci. U.S.A.* **107,** 20786–20791
52. Davis, I. W., Leaver-Fay, A., Chen, V. B., Block, J. N., Kapral, G. J., Wang, X., Murray, L. W., Arendall, W. B., 3rd, Snoeyink, J., Richardson, J. S., and Richardson, D. C. (2007) MolProbity: All-atom contacts and structure validation for proteins and nucleic acids. *Nucleic Acids Res.* **35,** W375–383